J|A|C|S
ARTICLES
Published on Web 03/22/2003

# Single, Double, and Multiple Double Strand Breaks Induced in DNA by 3−100 eV Electrons

Michael A. Huels,* Badia Boudaïffa, Pierre Cloutier, Darel Hunting, and Leon Sanche†

*Contribution from the Canadian Institutes of Health Research Group in Radiation Sciences, Department of Nuclear Medicine and Radiobiology, Faculty of Medicine, Université de Sherbrooke, Québec, Canada J1H 5N4*

Received November 29, 2002; E-mail: michael.huels@USherbrooke.ca

***Abstract:*** Nonthermal secondary electrons with initial kinetic energies below 100 eV are an abundant transient species created in irradiated cells and thermalize within picoseconds through successive multiple energy loss events. Here we show that below 15 eV such low-energy electrons induce single (SSB) and double (DSB) strand breaks in plasmid DNA exclusively via formation and decay of molecular resonances involving DNA components (base, sugar, hydration water, etc.). Furthermore, the strand break quantum yields (per incident electron) due to resonances occur with intensities similar to those that appear between 25 and 100 eV electron energy, where nonresonant mechanisms related to excitation/ionizations/dissociations are shown to dominate the yields, although with some contribution from multiple scattering electron energy loss events. We also present the first measurements of the electron energy dependence of multiple double strand breaks (MDSB) induced in DNA by electrons with energies below 100 eV. Unlike the SSB and DSB yields, which remain relatively constant above 25 eV, the MDSB yields show a strong monotonic increase above 30 eV, however with intensities at least 1 order of magnitude smaller than the combined SSB and DSB yields. The observation of MDSB *above* 30 eV is attributed to strand break clusters (*nano-tracks*) involving *multiple successive interactions* of one single electron at sites that are distant in primary sequence along the DNA double strand, but are in close contact; such regions exist in supercoiled DNA (as well as cellular DNA) where the double helix crosses itself or is in close proximity to another part of the same DNA molecule.

## Introduction

Although radiation therapy is the common mode of cancer treatment, there exists a persistent lack of fundamental knowledge of the complex, ultrafast reaction cascades that unfold on femtosecond time scales after the interaction of ionizing radiation with living tissue. The detailed knowledge of this unobserved sequence of nascent events, which is essential for the development of global models of cellular radiolysis and more efficient methods of radiotherapy, is achievable only by combining the results from low-energy electron and ion impact, synchrotron, and femtosecond laser experiments[1] on basic biomolecular model systems. It is known that when ionizing radiation deposits its energy in matter, it produces, within atto- to femtoseconds, large amounts of ions, radicals, excited neutrals, and ballistic secondary electrons with initial kinetic energies below 100 eV.[2−4] Subsequent reactions of these transients on short time scales may lead to substantial physical and chemical modifications of the medium, even within femtoseconds after the initial ionizing event; thus they determine the starting input for all the further, diffusion-limited, radiation chemistry and its eventual biological end-points.

The vast majority of the secondary electrons can induce further production of reactive anion and radical fragments via formation and decay of resonances, which also occurs on subpicosecond time scales. This has been shown to be the case for individual DNA/RNA components such as deoxyribose analogues,[5] DNA bases,[6−8] uracil[7] and its various radiosensitizing halogenated analogues,[9] small single-stranded oligonucleotides,[10] and hydration water.[11] Furthermore, in a recent preliminary study we found that low-energy electrons may also initiate strand break formation in double-stranded supercoiled DNA, even at energies as low as 4−6 eV.[12] Although our

† Canadian Research Chair in the Radiation Sciences.

(1) Research Needs and Opportunities in Radiation Chemistry Workshop, DOE Final Report SC-0003, US Department of Energy, 1998.
(2) *ICRU Report 31*, International Commission on Radiation Units and Measurements, Washington, DC 1979; and *ICRU Report 55*, 1995.
(3) Pimblott, S. M.; LaVerne, J. A. In *Radiation Damage in DNA: Structure/Function Relationships at Early Times*; Fuciarelli, A. F., Zimbrick, J. D., Eds.; Battelle Press: Columbus, OH, 1995; Chapter 1. LaVerne, J. A.; Pimblott, S. M. *Radiat. Res.* **1995**, *141*, 208.
(4) Cobut, V.; Frongillo, Y.; Patau, J. P.; Goulet, T.; Fraser, M.-J.; Jay-Gerin, J.-P. *Rad. Phys. Chem.* **1998**, *51*, 229.
(5) (a) Antic, D.; Parenteau, L.; Lepage, M.; Sanche, L. *J. Phys. Chem. B* **1999**, *103*, 6611. (b) Antic, D.; Parenteau, L.; Sanche, L. *J. Phys. Chem. B* **2000**, *104*, 4711.
(6) Huels, M. A.; Hahndorf, I.; Illenberger, E.; Sanche, L. *J. Chem. Phys.* **1998**, *108*, 1309.
(7) Hervé du Penhoat, M.-A.; Huels, M. A.; Cloutier, P.; Jay-Gerin, J.-P.; Sanche, L. *J. Chem. Phys.* **2001**, *114*, 5755.
(8) Abdoul-Carime, H.; Cloutier, P.; Sanche, L. *Radiat. Res.* **2001**, *155*, 625.
(9) (a) Abdoul-Carime, H.; Huels, M. A.; Illenberger, E.; Sanche, L. *J. Am. Chem. Soc.* **2001**, *123*, 5354. (b) Abdoul-Carime, H.; Huels, M. A.; Brüning, F.; Illenberger, E.; Sanche, L. *J. Chem. Phys.* **2000**, *113*, 2517.

measurements showed that the observed DNA damage is related to the type of electron resonances that are observed in small components of DNA, many important questions remain unanswered. The most immediate are (1) how do the strand break quantum yields (relative cross sections) involving electron resonances compare to those induced at higher electron energies where nonresonant mechanisms such as ionizations are believed to dominate, and (2) while low-energy (<15 eV) resonant electron damage to individual basic DNA components often involves complex bond cleavage and formation of reactive fragments, which in DNA may lead to a *solitary* single or double strand break, are electrons with higher energies (15−100 eV) able to induce more lethal and complex strand break clusters in DNA, due to their smaller *inelastic* mean free paths?

To address these questions, we have extended our ultrahigh-vacuum (UHV) techniques[12,13] developed recently for studies of low-energy electron beam damage to thin films of plasmid DNA. Furthermore, the goal was to obtain a self-consistent data set that allows us to directly compare the relative efficiency (cross section) of resonant electron damage to that induced by nonresonant electron impact phenomena at higher energies. Here we present the resulting measurements of single (SSB) and double (DSB) strand breaks, as well as the formation of short linear fragments of double-stranded DNA from supercoiled plasmid DNA, induced by 3−100 eV electrons under clean UHV conditions. The formation of short linear fragments requires creation of at least two or more DSB (i.e., a multiple DSB, viz., MDSB) occurring within the same plasmid; in the present study the length distribution of short linear fragments resulting from MDSB could not be further investigated, and their yields are reported as an integral value. However, experiments regarding the size distribution of DNA fragments resulting from MDSB are underway and will be published elsewhere.

Briefly, our present measurements on plasmid DNA films show that (1) for electron energies below 15 eV, formation and decay of well-localized transient anion states (resonances) within DNA is the *principal* mechanism leading to SSB and DSB. However, above 15 eV the electron energy dependent signature of the SSB and DSB quantum yields suggests that a superposition of nonresonant bond dissociation mechanisms is involved, namely, local electronic excitations, dissociations, or (dissociative) ionizations of the components of DNA, as well as multiple scattering energy loss of the incident high-energy electrons followed by (resonantly) induced strand break formation at a lower energy, and (2) 20−100 eV electrons are able to induce multiple strand break clusters in films of plasmid DNA in the form of MDSB (i.e., at least two DSBs in one plasmid), with yields that are at least an order of magnitude lower than the combined SSB and DSB yields over the entire electron energy range; however, in living cells such multiple double strand lesions are expected to be even more lethal and difficult to repair than a solitary SSB or DSB. The MDSB yields also appear to be dominated by nonresonant mechanisms and are believed to result from sequential ionization/dissociation/excitation events (nano-tracks) at sites that are distant in primary sequence within the plectonemically supercoiled plasmid, but are in close contact with each other. Since in irradiated matter nonthermal secondary electrons with initial kinetic energies below 15 eV outnumber those with higher energies[2−4] almost 10 to 1, we propose that in living cells most of the nascent DNA damage induced by the secondary electrons is dominated by the formation and decay of molecular resonances similar to those observed here, or previously in individual basic components of DNA.

## Experimental Methods

The experimental techniques developed for the present studies have been described in detail elsewhere.[12,13] Here we give only a brief description and note a few important aspects.

High-purity DNA solids are irradiated at ambient temperature under ultrahigh vacuum (UHV, $10^{-9}$ Torr) with a monoenergetic electron beam at various incident energies and total electron exposures ($\mathcal{E}$), with an energy resolution of 0.5 eV full width at half-maximum. The beam current is about 100 nA ± 1 nA. Exposure $\mathcal{E} \equiv ItA$, where $I$ is the current density of about $2.2 \times 10^{12}$ electrons $s^{-1}$ $cm^{-2}$, $t$ the time of irradiation, and $A$ the target area (about 6 mm diameter on average). A Faraday detector slit (0.3 mm wide) and phosphorescent plates are used to verify optimum spatial overlap between the DNA films (ca. 6 mm diameter on average) and the incident electron beam, which is collimated onto the target area via an in vacuo coaxial electromagnetic coil (20 Gauss). Uncertainties in the overlap between the electron beam and the target area $A$ are measured to be about ±5% of the target area radius and contribute the most to the experimental uncertainty in $\mathcal{E}$, which is estimated to be ca. ±10%. After electron irradiation, the DNA is dissolved in buffer and analyzed by agarose gel electrophoresis.

**Sample Preparation, Manipulation, and Post-irradiation Analysis.** Plasmid DNA (pGEM 3Zf(−), 3199 base pairs, ca. $1.9 \times 10^6$ amu per plasmid) is extracted from *E. coli* DH5α, purified, and resuspended in Nanopure water without any Tris or EDTA. All further sample manipulations occur in a sealed glovebox under a pure dry nitrogen atmosphere. An aliquot of the pure aqueous DNA solution is deposited onto chemically clean Ta substrates held at liquid nitrogen temperatures, lyophilized with a hydrocarbon-free sorption pump at 5 mTorr. Samples (10−12) are transferred directly to the UHV chamber without exposure to air or further characterization. Each sample consists of 500 ng of purified DNA in 10 μL of Nanopure water without any added salts and is deposited on the chemically clean Ta substrate over a measured area of about 6 mm average diameter. After lyophilization, this results in a solid calculated to be of 10 nm average thickness from a known density[14] of 1.7 g $cm^{-3}$, assuming minimal clustering of the plasmids in the solid. Since the average film thickness is smaller than either the effective range (12−14 nm) for damaging DNA with 10−50 eV electrons[13] or the penetration depth/mean free path (15−35 nm) of 5−100 eV electrons in liquid water or amorphous ice,[15] most of the electron beam is transmitted through the DNA films under single scattering conditions. After evacuation (∼24 h), each room-temperature DNA solid is irradiated individually with the electron beam; for each sample the time of irradiation, beam current density, and incident electron energy can be modified. Since during electron impact the irradiated sample is held at ground potential (in order to monitor the incident beam intensity), some of the secondary electrons produced at the surface, or backscattered incident electrons, may be emitted into the vacuum due to attractive fringe fields near the target; therefore, to prevent preirradiation, all other samples (to be irradiated later) are held at repulsive (negative) potentials.

(10) (a) Dugal, P.-C.; Huels, M. A.; Sanche, L. *Radiat. Res.* **1999**, *151*, 325. (b) Abdoul-Carime, H.; Dugal, P.-C.; Sanche, L. *Radiat. Res.* **2000**, *153*, 23. (c) Dugal, P.-C.; Abdoul-Carime, H.; Sanche, L. *J. Phys. Chem. B* **2000**, *104*, 5610.
(11) Rowntree, P.; Parenteau, L.; Sanche, L. *J. Chem. Phys.* **1991**, *94*, 8570.
(12) Boudaïffa, B.; Cloutier, P.; Hunting, D.; Huels, M. A.; Sanche, L. *Science* **2000**, *287*, 1658.
(13) Boudaïffa, B.; Cloutier, P.; Hunting, D.; Huels, M. A.; Sanche, L. *Radiat. Res.* **2002**, *157*, 227−234.
(14) Fasman, G. D. *Handbook of Biochemistry and Molecular Biology*, 3rd ed.; CRC Press: Boca Raton, FL, 1995.
(15) Meesungnoen, J.; Jay-Gerin, J.-P.; Filali-Mouhim, A.; Mankhetkorn, S. *Radiat. Res.* **2002**, *158*, 657.

After electron irradiation the samples are removed back into the dry nitrogen glovebox, where the DNA is dissolved in buffer (Tris-EDTA: 10 mM/1 mM; pH 7.5). Usually, about 95−98% of the deposited mass of plasmid DNA is recovered. Subsequently, the samples are analyzed by agarose gel electrophoresis and classified as supercoiled (SC, undamaged), relaxed, i.e., nicked circle (SSB), full length linear (DSB), and short linear forms (MDSB). The first three species produce distinct bands in the gels, and the latter produce a broad smear. The DNA held in solution contains 5% with SSB on average, and *none* with DSB or MDSB. Comparison of these control samples held in solution, with unirradiated samples held under UHV conditions for equivalent time periods, shows that deposition and recovery of plasmid DNA introduces only small amounts of additional SSB (∼8% on average) and *no detectable* DSB or MDSB. Quantitative analysis of DNA damage is performed using the ImageQuant program (Molecular Dynamics). For each scanned gel (i.e., sample) the fractional percent yields of SC, SSB, and DSB is obtained by integrating the area under the respective peaks representing the bands, whereas the percent yield of MDSB is determined from the integral of the entire broad feature representing the smear.

For each incident electron energy a typical exposure−response curve is obtained by irradiating about 8−10 identical samples at a fixed current density at increasing times of irradiation. This procedure is repeated five times at each incident electron energy and over the entire exposure time scale ($0 < t < 70$ min) under otherwise identical experimental conditions; thus for each incident electron energy about 40−50 samples are irradiated at different electron exposures, and a total of at least 800 samples have been irradiated for the measurements presented here. As described elsewhere,[12,13] *the quantum yields are then determined from linear least-squares fits to the initial slopes of the incident electron exposure−response curves* (in the very low exposure, *linear response regime*, $0 < t < 5$ min), at each incident electron energy, for SC loss, production of SSB, DSB, and MDSB. At each incident electron energy, the average slopes, obtained in the low exposure limit, are computed in units of percent yield per second and then converted to units of strand breaks per incident electron, as described elsewhere.[12,13] These quantum yields and their statistical standard deviations (reproducibilities) are then plotted versus incident electron energy for the entire electron energy range from 3 to 100 eV. They correspond to the *probabilities for induction of a particular damage by a single electron*; for example, at 11 eV incident electron energy a value of $(6.3 \pm 0.76) \times 10^{-4}$ SSB per incident electron means that about one out of 1580 electrons impinging on the thin DNA film produces a plasmid with at least one single strand break.

Finally, we first note two important aspects regarding the measurements presented here:

(1) In general the electron irradiations are performed on clean, freshly purified DNA, containing at least its structural water; this corresponds to about 2.5 water molecules per base pair,[16] such that the plasmid solids likely consisted of a mixture of A and C conformations. However, since our samples are not heated in the UHV, they may contain somewhat greater quantities of water in an adlayer, more typical of nonbaked (or nondegassed) vacuum surfaces. Furthermore, present DNA purification methods do not completely remove *all* salts or proteins strongly bound to the DNA, which may result in partial shielding and lowered sensitivity to DNA damage at the lowest electron energies, compared to the higher electron energies (however, *no* salts are added to the solutions in the film preparation). However, the small quantities of *residual* salts, proteins, and water tend to promote more uniform film coverage of the metal substrate during lyophilization (i.e., less clustering than from deposition of ultrapure DNA). All of these aspects are currently under investigation, and the measured quantum yields presented here are considered to be lower limits, particularly those measured at incident electron energies below 20 eV or near the apparent threshold of 4 eV for SSBs.

(2) The DNA damage reported here as SSBs and DSBs means that these plasmids have been converted under electron impact from a supercoiled to either a relaxed circular or full length linear conformation, respectively, as measured via gel electrophoresis. This means that they have received *at least one* SSB or *one* DSB, respectively. However, whether additional damage is present in these plasmids, particularly near the break site, e.g., base damage or deletion, oxidative damage, or even additional SSB, is not known at this time, but certainly warrants further study (this is also the case for surviving SC plasmids, which have no strand breaks, but may nonetheless possess types of localized damage sites, including base damage, etc., which are unobservable in gel electrophoresis).

For example a plasmid with one DSB will assume full length linear form even if one or more SSB is present in the same plasmid. Similarly a plasmid with a SSB will assume relaxed circular conformation even if a second SSB is present, as long as the second SSB is not within 10 base-pairs from the first, which actually would give rise to a DSB. We note that the cross section for the latter, i.e., conversion of a SSB to a DSB by a second arriving electron reacting within 10 base-pairs, has been determined with an empirical model[13] from electron exposure response data at 10, 30, and 50 eV to be at least 2 orders of magnitude smaller than direct formation of a DSB by a single electron event. Similar arguments apply to the MDSB yields, which represent short linear fragments, i.e., a plasmid that has received at least two (or more) DSB; whether the short linear fragments also possess additional SSB or base damage is not known. In either case the MDSB are reported as one integral value representing almost the entire range of linear fragment sizes in the smears observed in the gels; however, with the present method the smallest linear fragment observable consists of about 20 base-pairs, i.e., two turns of the DNA double helix.

## Results and Discussion

Figure 1a−c shows the measured yields (events per incident electron) for the induction of SSB, DSB, and MDSB in plasmid DNA induced by low-energy electron impact (3−100 eV). The independently measured yields of plasmids without any strand breaks (surviving SC) are not shown for clarity; however, we note that, within experimental uncertainty, they correspond to initial amount of DNA minus the sum of the SSB, DSB, and MDSB yields over the entire electron energy scale. At each electron energy, the error bars in Figure 1 correspond to the standard deviation of the average reported value, while the experimental uncertainty is about ±10%. We can clearly distinguish between different features appearing in the low incident electron energy region, i.e., below 15 eV (open symbols, Figure 1a,b), and those appearing in the high incident electron energy range between 15 and 100 eV (solid symbols, Figure 1a−c).

The SSB yields rise from an apparent threshold near 4−5 eV, whereas the DSB yield begins near 5−6 eV. Both yield functions possess a strongly peaked signature below 15 eV and have a broad peak (peaks) around 10 eV, a strong minimum near 14−15 eV (where the DSB yield is zero), a rapid increase between 15 and 30 eV, and above 30 eV roughly constant yields up to 100 eV. In stark contrast the MDSB yield has an apparent threshold near 18−20 eV and a very weak shoulder at 25 eV, above which it increases monotonically by about 1 order of magnitude up to 100 eV. At that electron energy the yield ratio of DSB to MDSB is about 3.4:1, but that for (SSB+DSB) to MDSB is 16:1. Together, these observations immediately suggest that the dominant mechanisms responsible for MDSB

(16) See for example: Swarts, S. G.; Sevilla, M. D.; Becker, D.; Tokar, C. J.; Wheeler, K. T. *Radiat. Res.* **1992**, *129*, 333.

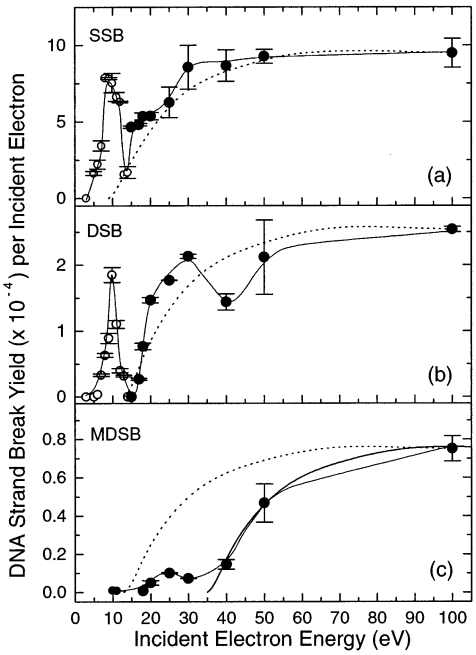


***Figure 1.*** Open and solid symbols are the measured quantum yields (events per incident electron) for the induction of SSB (a), DSB (b), and MDSB (c) in DNA films by low-energy electron impact, all shown as functions of incident electron energy; the solid curves through the data are guides to the eye. Each data point corresponds to an average of five exposure−response slope measurements, and the error bars represent one standard deviation of the average. The dotted curves symbolize general electron energy dependent signatures of cross sections for various nonresonant damage mechanisms, such as ionization cross sections, normalized here to the measured strand break yields at 100 eV (see text). In (c) such a curve shifted by 30 eV is also shown (heavy solid curve).

are likely to be very different from those responsible for either SSB or DSB.

Furthermore, we note that the peak SSB and DSB yields around 10 eV incident electron energy are similar in magnitude than their respective yields at 100 eV, and most importantly the maximum damage yield at that electron energy has not drastically changed in value from that near 30 eV.

In the remainder of this contribution we will discuss these and other aspects of our measurements, whereby we will consider the different DNA damage mechanisms most likely involved within the two distinct incident electron energy ranges, namely, that below 15 eV and that above 15 eV.

**DNA Damage below 15 eV: Resonant Mechanisms.** Shown in Figure 2a,b are the yields of DSB and SSB as functions of incident electron energy between 3 and 15 eV. Both yields show a very strong electron energy dependent signature, roughly characterized by an apparent threshold near 4−6 eV, a strong maximum between 7 and 13 eV, and a pronounced minimum between 14 and 15 eV; at that energy the DSB yield has dropped to zero.

Closer inspection of Figure 2 reveals that the DSB yield rises above 6 eV and has shoulders near 8 and 12.5 eV and a narrow peak at 10 eV. A multiple Gaussian fit to the DSB yield (dotted curve in Figure 2a) suggests three possible contributions (solid curves Figure 2a) to the general resonance profile at 8, 10, and 12.5 eV, with full widths at half-maximum (fwhm) of about 1.8, 1.7, and 1.4 eV, respectively. Conversely, the SSB yield shown in Figure 2b is found to have a much lower apparent threshold near 3−4 eV, a shoulder near 6 eV, and a very broad

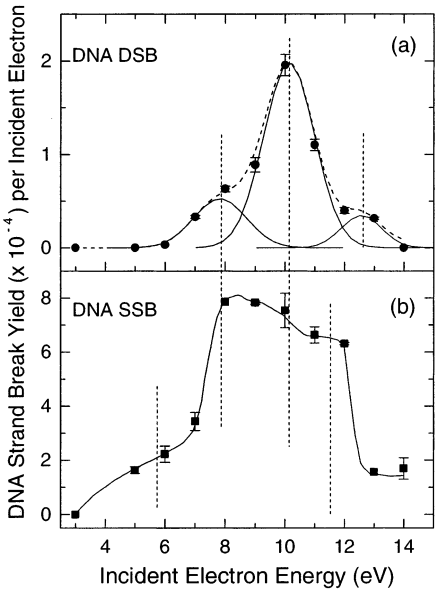


***Figure 2.*** Incident electron energy dependence of SSBs (solid squares) and DSBs (solid circles) below 15 eV. In (a) the dotted curve through the data points is a convolution of a multiple Gaussian fit to the data, consisting of at least three separate contributions (solid bell shaped curves), whereas in (b) the solid line through the data is a guide to the eye.

maximum centered around 10 eV, with a fwhm of about 5 eV. Although a multiple Gaussian fit to the SSB yield could not accurately reproduce the data (as for the DSB yields), it is estimated to contain contributions from unresolved features near 6, 8, 10, and 11.5 eV, as indicated by the vertical dotted lines.

Such pronounced peak signatures, seen here in the SSB and DSB yield curves for electron energies below 15 eV, have been previously observed in the anion yields obtained under electron impact at similar energies from gas or condensed phase DNA components[5−9] and water,[11] as well as in neutral base-fragment yields from single-stranded oligonucleotides[10] adsorbed on Au(111). These experiments, and reviews of current data,[17] clearly show that such peaks in the electron energy dependence of molecular fragmentation are associated with the formation of short-lived transient molecular anion (TMA) states of the molecule, i.e., resonances, followed by bond dissociation along one or several specific bonds.[5,6,8−10,18] For a molecule RH, e.g., as observed for films of deoxyribose analogues,[5] one of the many possible dissociative electron attachment (DEA) channels corresponds to

$$e^-(E) + RH \rightarrow (RH)^{*-} \rightarrow R^\bullet + H^- \quad (\text{or } R^- + H^\bullet, \text{ or other fragmentation channels}) \quad (1)$$

Depending on the excess energy of the dissociation process, the fragments may be ground or excited state atomic or molecular species (n*, v*, or l*), where the latter may themselves decay by dissociation along one or several bond coordinates. In larger polyatomic molecules, dissociation channels involving multiple bonds may also include complex bond rearrangements and significant nuclear motion[18] during the lifetime of the dissociating state, viz., "atom scrambling".

Alternatively, the TMA may also stabilize, or decay via electron autodetachment,[19] i.e.,

(17) Bass, A. D.; Sanche, L. *Radiat. Environ. Biophys.* **1998**, *37*, 243.
(18) Stepanovic, M.; Pariat, Y.; Allan, M. *J. Chem. Phys.* **1999**, *110*, 11376.

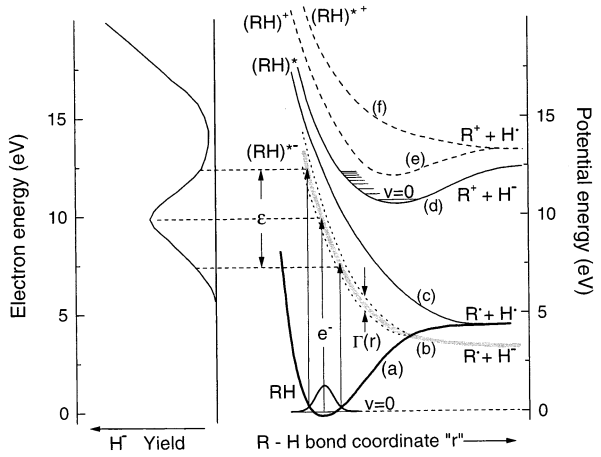


***Figure 3.*** Schematic Born−Oppenheimer potential energy curves involved in electron impact induced R−H bond cleavage via DEA (curve b) or nonresonant mechanisms (curves c−f); for discussion see the text. The left panel shows the $H^-$ yield that would result from DEA (the resonance peak) vs nonresonant dipolar dissociation (monotonically rising signal) above 14−15 eV.

$$e^-(E) + RH \rightarrow (RH)^{*-} \rightarrow (RH)^* + e^-(E' < E) \qquad (2)$$

where $(RH)^{*-}$ may be a dissociative or nondissociative state. In the former case, the autodetachment lifetime of the specific TMA state must be significantly shorter than the dissociation time for the electron to be emitted. Electron autodetachment may lead to an electron with lowered kinetic energy and a vibrationally and/or electronically excited (and possibly reactive) neutral molecule. Furthermore, depending on its energy and state, following (2) the excited state (RH)* may itself autodissociate into various neutral fragments, or a cation−anion pair, as observed for deoxyribose analogues.[5] In either case, damage induced by the (RH)* or its dissociation fragments would still retain much of the resonant signature of the initial electron attachment process. Thus, any DNA damage that is mediated by some type of resonance formation and decay (reaction 1 or 2) will essentially reflect the resonance signature.

Simple R−H bond cleavage is schematically illustrated in Figure 3, for the case of $H^-$ formation via DEA, by a Born−Oppenheimer potential energy diagram illustrating *resonant* electron attachment to a molecule RH in its electronic and vibrational ($\upsilon = 0$) ground state (curve a in Figure 3), leading to formation of a state $(RH)^{*-}$ with a repulsive potential (curve b in Figure 3) along the R−H bond coordinate "r". (In Figure 3 the excited state (RH)* formed by electron autodetachment from $(RH)^{*-}$ is not shown for clarity; it would lie below curve b and, if repulsive, could dissociate to an assymptote yielding ground state R + H or excited neutral fragments.) The probability for DEA and its yield signature are in part defined by the repulsiveness $\epsilon$ of the $(RH)^{*-}$ potential energy surface, as well as its uncertainty energy width $\Gamma(r) = \hbar/\tau$, where $\tau$ is the electron autodetachment lifetime (typically $10^{-14}$ to $10^{-13}$ s) of the TMA as given by the Heisenberg uncertainty principle. Thus, electron attachment is allowed via a vertical electronic transition to the state $(RH)^{*-}$ only at certain electron energies (Figure 3) for which there is sufficient Franck−Condon overlap between the nuclear wave functions of the initial ground state neutral and final anion states. As shown in Figure 3, this corresponds conceptually to a reflection of the RH($\upsilon$=0) nuclear ground state wave function (of Gaussian shape) by the repulsive potential energy surface $(RH)^{*-}$ and in part determines the peaked shape of the anion fragment yield, shown schematically in the left panel of Figure 3, for the example of $H^-$ formation via DEA to deoxyribose analogues.[5] Thus, if significant direct bond cleavage via DEA occurs in DNA, the strand break yields are expected to reflect these resonance signatures. The only other anion production mechanism is nonresonant dipolar dissociation, i.e., formation of a cation−anion pair (dipolar dissociation, neutral excitation to curve d in Figure 3), which will be discussed in the following section; in Figure 3 it gives rise to the monotonically rising $H^-$ signal above 13 eV.

The fundamental branching ratio between electron autodetachment and bond dissociation depends in part on the *intrinsic*[20] characteristics of the specific TMA (e.g., $\tau$, $\epsilon$, opening of new decay channels), whereas the final product or fragment yield in the condensed phase also depends on *extrinsic* effects[20] such as electron energy loss prior to resonant attachment, fragment reactions, or the conduction-band density of states of the solid, all of which depend on the structural and chemical composition of the immediate molecular environment. The latter will thus somewhat modify the resonant response of the pure individual components of DNA when localized within a DNA double strand; *therefore the DNA itself provides the physical and chemical environment for the localized resonant electron interactions with the individual DNA components.*

Shown in Table 1 are the peak positions observed in a variety of experiments in which either anion yields or neutral fragment yields were measured as functions of incident electron energy, from gas or condensed phase bases,[6−8] sugar analogues,[5] water,[11,21] or short segments of single-stranded DNA oligomers,[10] together with the electron energies at which peaks or structures are observed in the SSB or DSB yields in the present experiments. The comparison between these experiments shows that *all* DNA basic constituents, as well as small sections of single-stranded DNA, possess strongly dissociative resonances at incident electron energies at which the strand breaks are induced in large DNA molecules in the present experiments. Furthermore, the DEA fragmentation patterns observed in DNA components, or DNA oligomers, involve not only single but also multiple bond dissociations, all resulting in formation of highly reactive transients, which in turn may induce further localized damage. Therefore, the observation of DSB at incident electron energies well below those required for two ionizations (>20 eV) to occur within 10 bp of each other on opposing phosphate-sugar strands,[22] suggests that some fragmentation products may subsequently react locally with other DNA components and lead to a doubly damaged site with lesions on opposing strands. This is supported by the observation of electron-initiated fragment reactions (such as hydrogen abstraction, dissociative charge transfer, atom and functional group exchange, and reactive scattering) occurring over distances comparable to the DNA's double strand diameter (ca. 1−2 nm) in condensed films containing water[23] or small linear and cyclic hydrocarbons.[24]

(19) For DNA bases see: Aflatooni, K.; Gallup, G. A.; Burrow, P. D. *J. Phys. Chem. A* **1998**, *102*, 6205.

(20) (a) Huels, M. A.; Parenteau, L.; Sanche, L. *J. Chem. Phys.* **1994**, *100*, 3940. (b) Huels, M. A.; Parenteau, L.; Sanche, L. *Chem. Phys. Lett.* **1997**, *279*, 223.

(21) Curtis, M. G.; Walker, I. C. *J. Chem. Soc., Faraday Trans.* **1992**, *88*, 2805, and references therein.

(22) Hieda, K. *Int. J. Radiat. Biol.* **1994**, *66*, 561.

***Table 1.*** Incident Electron Energy Ranges (eV) at Which Maxima in Specific Molecular Damages Are Observed in DNA and Its Basic Constituents[a]

| compound | 4–7 | 7.5–8.5 | 9–11 | 11.5–13 | 14–15 | 18–23 | 25 | 30 |
|---|---|---|---|---|---|---|---|---|
| DNA (present work) | ssb(6) | ssb(8) | ssb(10) | ssb(11.5) | | ssb(19) | (msb) | ssb |
| | | dsb(8) | dsb(10) | dsb(12.5) | | dsb(22) | | dsb |
| oligomer single-strand[10] | | | $CN^{\bullet}$ | $CN^{\bullet}$, $OCN^{\bullet}$, $H_3C-CCO^{\bullet}$ | | | | |
| adenine (solid)[8] | | | $H^-$, $CN^-$ | | $CN^-$ | $H^-$ | $CN^-$ | |
| guanine (solid)[8] | | | $H^-$, $CN^-$, $O^-$ | $OH^-$ | $CN^-$, | $H^-$, $CN^-$, $O^-$, $OH^-$ | | |
| thymine (solid)[8,7] | | ($O^-$), ($OCN^-$) | $H^-$, $CN^-$, $O^-$, $OH^-$, $CH_2^-$ | $O^-$, $OCN^-$, | $CN^-$, | $H^-$, $CN^-$, $OH^-$, $OCN^-$, $CH_2^-$ | | |
| thymine (gas)[6] | $OCN^-$, $CN^-$, $OCNH^-$, $O^-$, $H^-$, $OCNH_2^-$ $CH_2^-$ | $OCN^-$, $CN^-$, $OCNH^-$, $O^-$, $H^-$, | | | | | | |
| cytosine (solid)[8] | | $O^-$ | $H^-$, $CN^-$, $OH^-$ | | | $H^-$, $CN^-$ | | |
| cytosine (gas)[6] | $OCN^-$, $H^-$, $CN^-$, $O^-/NH_2^-$, $C_4H_5N_3^-/C_4H_3N_2O^-$, $C_4H_3N_2^-$ | $OCN^-$, $CN^-$, $O^-/NH_2^-$, $C_4H_5N_3^-/C_4H_3N_2O^-$, $C_4H_3N_2^-$ | $H^-$, $O^-/NH_2^-$, | | | | | |
| deoxyribose (solid)[5] | | | $H^-$ | | | $H^-$ | | |
| $H_2O$ (gas)[21] | | $H^-$ (+OH) | $H^-$ (+OH) | | | | | |
| $H_2O$ (solid)[11] | | $H^-$ (+OH) | $H^-$ (+OH) | | | | | |

[a] Numbers in parentheses denote peak energies in eV; superscripts indicate the reference from which the data were obtained.

Thus, based on the observed resonance peaks and structures in the DNA damage yield below 14 eV (Figures 1 and 2, Table 1), *we propose that localized resonance formation and decay involving individual basic DNA units occur inside the plasmid DNA and lead to final strand lesions*. The various resonances of the individual DNA components will contribute with different statistical weight to the final yield of DNA damage observed here, which therefore represents a superposition of the numerous resonance channels involving the basic DNA components, as well as the subsequent localized reaction cascades involving the transient reactive species formed by the resonance decay. Although at the present we cannot unravel which resonance of which basic DNA component contributes to SSBs or DSBs at a given energy, we note that (a) the DSB yield appears to be dominated to a large extent by probably a single resonance at 10 eV, which coincides with the $H^-$ DEA peak from deoxyribose analogues (Table 1), and (b) the SSB yield peak is much broader and appears to be related to possibly three resonances contributing with similar statistical weight to the SSBs.

**DNA Damage between 15 and 100 eV: Nonresonant Mechanisms and MDSB.** As shown in Figure 1, above 15 eV we note that (a) both the SSB and DSB yields rise monotonically from an apparent threshold and reach a plateau near 30 eV, (b) the SSB and DSB yields at 30−100 eV have intensities similar to their respective values at 10 eV, where resonant mechanisms occur, and (c) the MDSB yield has a small structure near 25 eV, rises monotonically above 30 eV, and appears to reach a plateau near 50−100 eV. In the following, we will examine the likely mechanisms that may lead to the observed DNA damage at such energies, including possible contributions of secondary electrons, produced here by the higher energy incident electrons, and thereby attempt to interpret the results.

At the present electron energies (even below 15 eV) many nonresonant mechanisms exist that can contribute to the observed DNA damage, such as transitions to excited states of the neutral molecule or its cations (curves c−f in Figure 3). Nonresonant, direct scattering excitations of a DNA component, i.e.,

$$e^-(E) + RH \rightarrow (RH)^* + e^-(E' < E) \qquad (3a)$$

may lead to formation of a neutral excited transient, which is itself reactive, or to formation of reactive fragments from the excited neutral via subsequent bond cleavage along a number of different dissociation pathways. The thermodynamic threshold energies for subsequent dissociation of (RH)* within the solid corresponds to the lowest dissociation energy of the various electronically excited state (RH)* which can produce at least two neutral radicals, e.g., $R^{\bullet} + H^{\bullet}$ (e.g., curve c in Figure 3), or a cation−anion pair, e.g., $R^+ + H^-$ (curve d in Figure 3), screened by the polarization they induce in the solid (viz., dipolar dissociation, DD), i.e., respectively

$$(RH)^* \rightarrow R^{\bullet} + H^{\bullet}, \text{ etc., or } R^+ + H^-, \text{ etc., or } R^- + H^+, \text{ etc.} \qquad (3b)$$

The thermodynamic thresholds for dissociations yielding only neutral fragments depend on the average bond dissociation energies ($D°$) of the DNA components, i.e., at least about 4 eV on average, but will likely require some additional excitation/activation energy to be formed by electron impact (e.g., curve c in Figure 3); dissociation yielding $R^+ + H^-$, or $R^- + H^+$, fragments will require a minimum energy equivalent to $D° + IP - EA$, where IP is the lowest ionization potential, and EA the electron affinity of a given fragment. The lowest IPs of DNA

(23) Sieger, M. T.; Simpson, W. C.; Orlando, T. M. *Nature* **1998**, *394*, 554.
(24) (a) Bass, A. D.; Parenteau, L.; Huels, M. A.; Sanche, L. *J. Chem. Phys.* **1998**, *109*, 8635. (b) Huels, M. A.; Parenteau, L.; Sanche, L. *Chem. Phys. Lett.* **1997**, *279*, 223.

components are found near 8 eV for guanine,[25] 6.5 eV for a stacked GC base pair, 5.7 eV for a fully "solvated" GC base pair,[26] and 10−11 eV for B- and Z- sugar−phosphate backbone fragments,[27] whereas the EAs of DNA base pairs are calculated around 0.7−1.6 eV for GC or AT pairs (electrons localized on C or T, respectively) or 1−1.3 eV for fully "solvated" GC base pairs.[26] It should be noted that unlike for reaction 2, viz., resonance-enhanced neutral excitation, in reactions 3a,b the electron energy dependence of the (RH)* formation cross section will not involve resonance features, since here temporary capture of the incident electron is not involved and the scattering process is of a direct nature.

Similarly, single ionization with or without dissociation (e.g., curve e or f in Figure 3) may lead to formation of reactive transients via

$$e^- + RH \rightarrow (RH)^+ + 2e^-, \quad (4)$$

or

$$e^- + RH \rightarrow (RH)^{*+} + 2e^- \quad (5a)$$

followed by

$$(RH)^{*+} \rightarrow R^\bullet + H^+, \text{ or } R^+ + H^\bullet, \text{ or others} \quad (5b)$$

The cross sections for most materials, including organic molecules, are expected to be in the $10^{-16}$ cm$^2$ range; for example, typically for gas phase methane near 70 eV they are found to be about $1.6 \times 10^{-16}$ cm$^2$ for reaction 4 and about $2.3 \times 10^{-16}$ cm$^2$ for the sum of all fragmentation channels 5a,b.[28] If the positive ion $(RH)^+$ is created in a highly dissociative state $(RH)^{*+}$, a cation and a radical fragment are formed with nonthermal energies and may induce further damage. In principle, the thermodynamic thresholds for reaction 4 in DNA may be as low as about 6 eV,[26] while for reactions 5a,b thresholds would increase by the average $D°$ in a DNA component, i.e., about 4 eV on average.

Although multiple ion fragment formation, e.g.,

$$e^- + RH \rightarrow R^+ + H^+ + 3e^- \text{ or other fragmentation channels} \quad (6)$$

are generally possible at the current electron energies below 100 eV, their total cross sections in DNA components are likely to be 2 orders of magnitude smaller than those for either reaction 4 or 5a,b, at least based on available methane gas phase data.[29]

Thus, neutral dissociations, excitations, and single and multiple ionizations (i.e., reactions 3−6) in DNA may lead to bond cleavage and in principle should contribute to the SSB and DSB yields at any energy above their respective thermodynamic thresholds. *However*, the incident electron energy dependence for *any* of these *nonresonant* mechanisms (3−6) will be distinguished by a signature similar to that for ionization processes, the cross sections for which are generally characterized by a monotonically rising signal above a thermodynamic threshold[30] and a broad peak at higher energies (near 70−100 eV[30−33] for ionization processes). This is because unlike DEA, which requires a specific Franck−Condon overlap between the neutral and anion state for the initial electron capture and is allowed only for a range of specific electron energies for a given $\Gamma(r)$ and $\epsilon$ (transition from curve a to b in Figure 3), all nonresonant direct excitations of the neutral or its cation (curves c−f in Figure 3) are allowed at any energy above threshold in the Franck−Condon region and include the manifold of continuum states for each specific excitation. Thus, the formation of DNA strand breaks via different nonresonant excitation and ionization events in the medium would be expected to follow a convolution of many such nonresonant, monotonically rising signatures.

The typical shape of such a nonresonant signature is schematically exemplified by the dotted curves in Figure 1a−c, which are taken from the total ionization cross sections (including dissociative ionizations) in gas phase methane that have been normalized here at 100 eV to the respective strand break yields. The thresholds for these curves have been set to about 8 eV for SSBs and about 13 eV for DSBs in order to account for the minima in the measured strand break yields near 14−15 eV: if nonresonant mechanisms would contribute substantially to the strand break yields at significantly lower thresholds (e.g., 5.7−6.5 eV for the IP of GC base pairs), the resonant signatures observed in the strand break yields would be superimposed below 15 eV on a much higher monotonically rising background signal, with the minima at 15 eV being less deep than observed here (e.g., here the DSB yield goes to zero near 14 eV). Therefore, the first two points to be noted are (a) for electron energies below 15 eV, mechanisms involving formation and decay of resonances appear to dominate the SSB and DSB yields, and (b) above 15 eV the electron energy dependence of the SSB and DSB yields is on the whole in qualitative agreement with a generalized monotonically rising signature expected for a manifold of nonresonant mechanisms. This suggests that a superposition of nonresonant excitations, dissociations, and ionizations is likely responsible for most of the observed SSBs and DSBs between 15 and 100 eV.

We find nevertheless that the measured SSB and DSB yields above 15 eV show some structured fluctuations from this generalized signature for nonresonant mechanisms, notably the drop in DSB yield near 40 eV (and apparent structure near 25−30 eV) and weak structures in the SSB yield near 19 and 30 eV. Whether or not they are related to multiple scattering electron energy loss (EEL), followed by resonance formation

(25) Sevilla, M. D.; Besler, B.; Colson, A.-O. *J. Phys. Chem.* **1995**, *99*, 1060.
(26) Colson, A.-O.; Besler, B.; Sevilla, M. D. *J. Phys. Chem.* **1993**, *97*, 13852.
(27) Colson, A.-O.; Besler, B.; Sevilla, M. D. *J. Phys. Chem.* **1993**, *97*, 8092.
(28) Straub, H. C.; Lin, D.; Lindsay, B. G.; Smith, K. A.; Stebbings, R. F. *J. Chem. Phys.* **1997**, *106*, 4430.
(29) Lindsay, B. G.; Rejoub, R.; Stebbings, R. F. *J. Chem. Phys.* **2001**, *114*, 10225.
(30) Massey, H. S. W.; Burhop, E. H. S.; Gilbody, H. B. *Electronic and Ionic Impact Phenomena*, Vol. II, *Electron Collisions with Molecules and Photoionization*; Massey, H. S. W., Ed.; Clarendon Press: Oxford, 1969.
(31) For all known materials (in the gas phase), the electron impact single ionization cross sections show a smoothly rising signal above a threshold and a peak near 70−100 eV, above which the cross sections decrease slowly for increasing electron energies into the keV range. This is similar for double or multiple ionization cross sections, for which the peak shifts to successively higher electron energies, as well as for ionization cross sections involving molecular fragmentation, e.g., see ref 28. Nonresonant cross sections for dissociation into neutral fragments exhibit a broad peak in the 20−50 eV range, depending on the excited state involved (e.g., Märk, T. D.; Hatano, Y.; Linder, F. In *Atomic and Molecular Data for Radiotherapy and Radiation Research*; IAEA TECDOC-799 Research Program Report; 1995; Chapter 3). In solid or liquid media, aside from multiple scattering phenomena and other bulk effects (such as conduction band density of states, etc.), the electron energy dependence of the fundamental nonresonant ionization/dissociation mechanisms is usually found to be generally similar to those in the gas phase.
(32) Straub, A. C.; Linsay, B. G.; Smith, K. A.; Stebbings, R. F. *J. Chem. Phys.* **1998**, *108*, 109.
(33) Pimblott, S. M.; La Verne, J. A.; Mozumder, A. *J. Phys. Chem.* **1996**, *100*, 8595.

at lower energies, cannot be ascertained at this time, since EEL spectra for DNA at such low incident electron energies are not available. However, we note that evidence for multiple scattering EEL and vibrational and electronic excitations exists in physisorbed water[34] and many other organic films[35] including DNA base[36] and deoxyribose analogues,[37] and is known to somewhat enhance molecular fragmentation yields at energies near 20−30 eV, e.g., via EEL excitations followed by DEA,[20a,38] but may not exceed direct DEA fragment yields by equivalent lower energy electrons. This is because the final cross section (i.e., probability) for EEL followed by DEA is determined by the product of the individual probabilities (each $\ll 1$) and can never be greater than any one individual probability for either EEL or DEA. Furthermore, since the penetration depth[15] or range[13] of 3−100 eV electrons is larger than the present film thickness (10 nm), most electrons interact only once in the films, and many electrons that undergo an energy loss event in the film bulk will likely end up in the metal or escape into the vacuum. Thus, a strand break induced in a specific plasmid via EEL of the incident higher energy electrons (i.e., via ionization, excitation, dissociation leading to a strand break) followed by a strand break in *another* plasmid at lowered energy has an overall reduced probability and is not likely to dominate or substantially enhance the SSB and DSB yields observed in the present thin films. Alternatively, as discussed in the experimental method, if in one specific plasmid a strand break is induced via an EEL process of the incident electron, a subsequent strand break induced *in the same plasmid by the same electron* with lowered energy will not always be distinguishable as such. (This also applies to damage induced by a primary and its secondary electrons in the same plasmid: the general notion that successive damage events induced in the present thin films by either the incident electrons or the secondary electrons have low probability is supported by the low yields of MDSB, which will be discussed shortly.)

The third point to be noted here is that, for example, at 100 eV, the SSB or DSB yield intensities possess magnitudes similar to their respective values near 10 eV. This suggests that in the present DNA films the total contribution of all nonresonant mechanisms, available to the incident 100 eV electron (and the secondary electrons created by them), to the SSBs or DSBs yields is similar to the total contribution of all resonant mechanisms by which a 10 eV incident electron can initiate damage to DNA. If we neglect for a moment any secondary electrons that may be formed by a 100 eV incident electron, then the total cross section for a certain type of DNA damage, e.g., direct SSB formation by the incident electron in a single event, is the sum of all possible individual cross sections for excitations (leading to reactive transients), neutral dissociations, and ionizations (with or without dissociation), involving the various individual components of the DNA plasmid, i.e., reactions 3−6 each with individual cross sections likely in the $10^{-18}$ to $10^{-16}$ cm$^2$ range. Thus, for the direct SSB yield at 100 eV to be similar to the 10 eV SSB yield requires only that the sum total of all the individual cross sections for strand breaks initiated via resonant electron attachment to the various DNA components, e.g. DEA- or resonant-enhanced excitation (reactions 1 and 2), be similar in magnitude than the total nonresonant cross section at 100 eV. This is in fact not unreasonable if we consider (a) the great number of different DEA-induced fragmentation pathways observed in basic DNA components (Table 1), and (b) the fact that gas phase DEA cross sections, which, for example, for individual DNA bases or amino acids already range near $(3-30) \times 10^{-16}$ cm$^2$,[6,39] are usually *enhanced* in the condensed phase[40] due to charge-induced polarization effects of the molecular environment (i.e., the plasmid DNA) on the transient anion state. Here polarization of the surrounding medium by the transient anion tends to increase the electron autodetachment lifetime of the anion state, allowing more time for dissociation or stabilization. Since many of the nonresonant mechanisms of fragmentation involve an intermediate *neutral* excited state or, in the case of ionizations, have no other competing channels (other than cation−secondary electron recombination, which is less probable here since the hole is likely to quickly enter the metal due to attraction by the image charge), their cross sections are not expected to be enhanced significantly by this mechanism.

Consequently, the remaining question is to what extent secondary electrons contribute to the SSB or DSB yields (at higher incident electron energies, e.g., 100 eV), since they may in principle also ionize or dissociate molecules, undergo EEL, or even induce DEA, depending on the kinetic energy with which they are created. Although the *G*-value for production of secondary electrons in bulk water,[2,4] 4−5/100 eV deposited, might suggest that here in DNA a 100 eV electron may generate similar quantities of secondary electrons, this is not likely to be the case: *G*-values for secondary electron production involve high-energy (keV−MeV) primaries in bulk organic media, whereas the present experiments involve low-energy primaries in DNA films that are thinner than the average penetration depth[15] (or mean free path) of 3−100 eV electrons, which are likely to interact only once while traversing the film. Thus, the number of secondary electrons created here by the incident electrons during their passage through the thin film will be substantially less. Using a primitive approximation,[41] we may roughly estimate the yield of secondary electrons produced in the thin DNA films to have an upper limit of about 0.15−0.6 per incident electron above 30 eV, i.e., at most about one secondary electron per two incident electrons. Below 30 eV this number drastically decreases with decreasing electron energy, due to the rapid decrease of the ionization cross sections near threshold. (This also means that particularly below 15 eV incident electron energy the number of secondary electrons that may contribute to strand breaks is negligible, and thus the SSB and DSB yields below 15 eV are dominated by *single incident*

(34) (a) Michaud, M.; Sanche, L. *Phys. Rev. A* **1987**, *36*, 4672. (b) Michaud, M.; Sanche, L. *Phys. Rev. A* **1987**, *36*, 4684. (c) Michaud, M.; Cloutier, P.; Sanche, L. *Phys. Rev. A* **1991**, *44*, 5624. (d) For multiple scattering theory in molecular films see also: Michaud, M.; Sanche, L. *Phys. Rev. B* **1984**, *30*, 6067.
(35) For example: (a) Swiderek, P.; Michaud, M.; Sanche, L. *J. Chem. Phys.* **1993**, *98*, 8397. (b) Swiderek, P.; Michaud, M.; Sanche, L. *J. Chem. Phys.* **1995**, *103*, 8424. (c) Swiderek, P.; Michaud, M.; Sanche, L. *J. Chem. Phys.* **1996**, *105*, 6724.
(36) (a) Crew, A. V.; Isaacson, M.; Johnson, D. *Nature* **1971**, *231*, 262. (b) Isaacson, M. *J. Chem. Phys.* **1972**, *56*, 1803. (c) Dillon, M. A.; Tanaka, H.; Spence, D. *Radiat. Res.* **1989**, *117*, 1.
(37) Lepage, M.; Letarte, S.; Michaud, M.; Motte-Tollet, F.; Hubin-Franskin, M.-J.; Roy, D.; Sanche, L. *J. Chem. Phys.* **1998**, *109*, 5980.
(38) Sambe, H.; Ramaker, Parenteau, L.; Sanche, L. *Phys. Rev. Lett.* **1987**, *59*, 505.
(39) Gohlke, S.; Rosa, A.; Illenberger, E.; Brüning, F.; Huels, M. A. *J. Chem. Phys.* **2002**, *116*, 10164.
(40) (a) Sambe, H.; Ramaker, D. E.; Deschenes, M.; Bass, A. D.; Sanche, L. *Phys. Rev. Lett.* **1990**, *64*, 523. (b) Ayotte, P.; Gamache, J.; Bass, A. D.; Fabrikant et, I. I.; Sanche, L. *J. Chem. Phys.* **1997**, *106*, 749−760.

*electron events involving resonances* of DNA components.) If we assume that the kinetic energy distributions of secondary electrons produced here by 30−100 eV incident electrons is similar to those calculated for higher energy incident electrons in water or DNA,[2−4] then about 58% of the secondary electrons will have kinetic energies below 6 eV and will not contribute significantly to the SSB or DSB yields, while 25% have energies between 6 and 13 eV, and 17% have energies above 13 eV. Thus, the fraction of secondary electrons that have sufficient energy above 6 eV to contribute to the measured SSB or DSB yields via resonant or nonresonant mechanisms is at most 0.06−0.25 per incident electron above 30 eV, *or at most one secondary electron per four incident electrons*. The notion that this value is indeed an upper limit is also suggested by the recent observation[42] that the cross sections for inelastic scattering (including ionization) by 1−100 eV electrons in amorphous ice is 3.5 times smaller than in water vapor; if this is generally the case for molecular films, then here the yield of secondary electrons with more than 6 eV kinetic energy would be below 0.08 per incident electron above 30 eV.

Moreover, similar to the 3−100 eV incident (primary) electrons, in solid media the penetration depths[15] (or mean free paths) of the secondary electrons with energies above 6 eV, i.e., 15−35 nm, are larger than the present film thickness (10 nm). This implies that most of the secondary electrons produced deeper in the bulk somewhat near to the metal substrate are expected to leave the film, since they are strongly attracted toward their image charge in the metal and will not likely contribute to damage in *another* plasmid, due to their long range. Conversely, a further fraction (possibly half) of the secondary electrons produced near the film/vacuum interface may scatter out into the vacuum (this is in part due to the isotropic nature of secondary electron emission and because during irradiation the samples are not held at an attractive potential to trap all secondary electrons produced at the surface). However, since the fraction of secondary electrons that are lost from the films cannot be accurately determined at this stage, we estimate that here the overall contribution of secondary electrons to the measured SSB or DSB yields is no greater than about 20−25% for incident electron energies above 30 eV; below that energy the contribution of secondary electrons is believed to be negligible, particularly below 15 eV. In other words, even if all secondary electrons (i.e., the 0.25 per incident electron) formed at 100 eV would remain in the film, and for some reason all possess 10 eV kinetic energy, thus inducing damage via the efficient DEA mechanism, their contribution to the SSB or DSB yields at 100 eV would be no more than 25% of the equivalent yield (per incident electron) measured at 10 eV.

(41) Although only valid in low- to high-pressure gases, we may use the Lambert−Beer law to estimate an upper limit of secondary electrons produced here in the thin organic films: the ratio of cations ($n_i$) (which is proportional to the number of secondary electrons, $n_2$) to incident electrons ($n_o$) produced by single ionization relates to the number of electrons ($n$) that have not experienced an ionizing collision in the film, via $(n_2/n_o) = (n_i/n_o) = 1 - (n/n_o) = 1 - \exp\{-NL\sigma_i\}$, where $N$ is the target number density in the film of thickness $L$ ($\approx$10 nm $= 10^{-6}$ cm) and $\sigma_i$ is the ionization cross section (here we use a typical *average* cross section of about $10^{-16}$ cm$^2$, for single ionization by 30−100 eV electron impact to most gas phase molecules). For the present 500 ng films (film area $\approx$ 0.3 cm$^2$), the density of DNA plasmids ($3.1 \times 10^{-18}$ g/plasmid) is about $5.3 \times 10^{17}$ plasmids/cm$^3$; thus, if the density of ionizable target units in the DNA plasmid film is given by the number of nucleotide pairs in the film (3199/plasmid, i.e., $N \approx 1.7 \times 10^{21}$/cm$^3$), then $(n_2/n_o) \approx 0.15$, whereas if the targets are defined as either the individual base, sugar, phosphate, or water units ($N \approx 10^{22}$/cm$^3$), then $(n_2/n_o) \approx 0.6$.

(42) Michaud, M.; Wen, A.; Sanche, L. *Radiat. Res.*, in press.

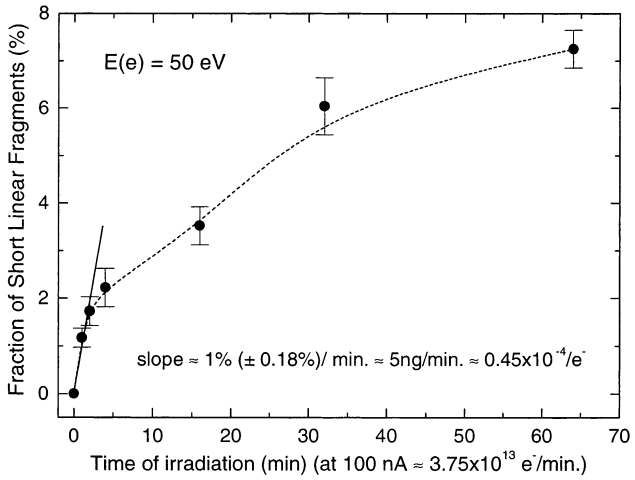


***Figure 4.*** Typical exposure−response curve for the formation of short linear fragments (MDSB) from plasmid DNA, here by 50 eV electron impact, at a constant electron beam flux for increasing electron exposure times. The slope of the linear fit to the data at the earliest exposure times determines the quantum yield per incident electron, as described elsewhere;[12,13] the dotted line is a guide to the eye.

Finally, we note that any secondary electron that does contribute to damage in *the same* plasmid in which it is produced will not be distinguishable or contribute to the next higher type of damage (see discussion on EEL). In any case, the small yield of secondary electrons would be expected to follow ionization cross sections, i.e., a monotonically rising signal above a thermodynamic threshold. Thus at energies above 15 eV the total density of reactive transients, including secondary electrons, produced by the convolution of all mechanisms would increase monotonically with incident electron energy, causing a similar monotonic increase in DNA strand breaks.

As shown in Figure 1c, unlike the SSB and DSB yields above 15 eV, the MDSB yields do not follow a generalized signature representative of single nonresonant events such as ionization. A typical MDSB electron exposure−response curve obtained at 50 eV is shown in Figure 4.

Here, the MDSB yield rises linearly at very early exposure times *before* a substantial accumulation of full length linear form has occurred. Thus, as given by the example in Figure 4, the linear fit to the exposure−response data below 4 min exposure is used (as described previously[12] for DSBs and SSBs) to determine the MDSB quantum yields (MDSB per incident electron) shown in Figure 1c. Unless otherwise stated, these values are obtained on exposure time scales where the DSB and SSB exposure−response yields are also linear, indicating single electron events.

We therefore propose that the formation of MDSBs involves direct interactions of a single incident electron with multiple sites in a single DNA molecule. In general, this is possible if regions of the DNA, which are distant in primary sequence along the DNA double strand, are in close contact as discussed previously[43] (i.e., where the DNA helix crosses itself or is in close proximity to another part of the same DNA molecule). Thus, the deposition of sufficient energy in a small volume by low-energy electrons may result in the formation of at least two DSBs which are separated by hundreds or thousands of base pairs along the primary sequence. This is supported by recent

(43) Boudaïffa, B.; Cloutier, P.; Hunting, D.; Huels, M. A.; Sanche, L. *Int. J. Radiat. Biol.* **2000**, *76*, 1209.

calculations of the different plectonemic conformations of DNA,[44] which show that minimized energy configurations of supercoiled plasmid DNA may contain sites where the double strand crosses itself at least once, or more, in either a standard figure eight conformation or various knotted shapes.

Below 30 eV, the MDSB yields in Figure 1c show a weak structure near 25 eV, which may involve the formation of a TMA. One of many possible scenarios for this structure in the MDSB yield may involve a two-step mechanism similar to that observed near 20 eV electron energy in films of deoxyribose analogues:[5] here the incident electron is captured into a high-energy TMA state of a basic DNA component, which decays by electron autedetachment into a *dissociative* neutral excited state; this results in, for example, formation of a reactive anion and cation fragment, and thus a DSB. Subsequently, the detached electron (with reduced energy) may now in the same plasmid induce a further DSB by DEA to another DNA component at a lowered energy. Nevertheless, we note that at 30 eV and below MDSB fragment signals appear only after a short preirradiation of 2−3 min, i.e., when small quantities of DSBs have already begun to accumulate; however, after the short preirradiation, the MDSB exposure−response signal does rise linearly for additional exposures between 2 and 5 min. Thus, only in the case of MDSBs at 30 eV and below do we find possible contributions related to film degradation. In that sense, the weak structure seen here in the MDSB yield near 25 eV (Figure 1c) may also relate to a resonance of the full length linear plasmid that has been produced by the impact of a previous incident electron.

We find that the electron energy dependence of MDSB yield between 40 and 100 eV roughly fits a nonresonant type monotonically rising signature, similar to ionization cross sections, but for which the threshold has been shifted to about 35 eV (solid curve in Figure 1c); although the true threshold cannot be determined here, it probably lies closer to 30 eV. Since the measured apparent threshold for DSB formation via nonresonant ionizations/excitations by a single electron is about 15 eV (see Figures 1c and 2b), this suggests that the formation of MDSBs requires sufficient energy of the incident electron, equivalent to that needed for at least two discrete "hits" inducing two DSBs. This would be equivalent to DSB formation with EEL, followed by the second DSB induced by the same electron in the same plasmid (as discussed previously). Although in the present experiments the size distribution of the short linear fragments could not be determined, the measurements nonetheless show that a large smooth spectrum of fragment size distributions is formed, i.e., a broad smear in the gels. This implies that, at least at 40 eV and above, more than two DSBs can be induced in the same plasmid by one incident electron, with proportionally increasing thresholds for three, four, etc., successive hits (i.e., EEL events) by the same incident electron at different sites in the plectonemically wound plasmid, i.e., a track of nanometer dimensions.

However, in the present experiments we can only state with certainty that *at least two* DSBs have occurred in one plasmid, e.g., where the helical strands cross; thus, an alternative interpretation could be that a single incident electron deposits probably all of its energy in the small region where the strands cross and generates sufficient initial bond cleavage *as well as* numerous transient reactive species; the latter immediately interact in a cascade with the various DNA components in the vicinity of the strand crossing site, thus resulting in at least two DSBs that are adjacent to each other, but distant in base sequence. Such a single event would be similar to that of Coulomb explosions,[45] as observed in condensed phase water[46] or methane[47] under keV electron impact, where the *inter*molecular Coulomb explosions are associated with delocalization of valence holes related to bonding C−H orbitals, leading to enhanced cation fragment yields, in addition to fragmentation induced by dissociative ionization. In the present case, DNA plasmid *intra*molecular Coulomb explosions would involve hole delocalization of adjacent DNA components or residual hydration water.

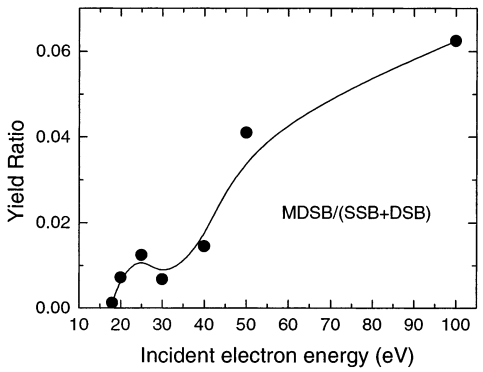


***Figure 5.*** Incident electron energy dependence of the yield ratio of MDSB/(SSB+DSB); the solid curve is a guide to the eye. Exposure−response analysis indicates that below 40 eV only the MDSB yields may contain some contribution from degradation of the DNA films by successive incident electrons; however, at 40−100 eV the MDSBs are the sole result of multiple events involving a single incident electron (see Figure 4).

In either case, successive isolated EEL events along a short single electron track or one single violent energy deposition at a strand crossing, the measured MDSB yields are significantly smaller, i.e., by 2 orders of magnitude, than the total SSB and DSB yield below 30 eV, as shown in Figure 5. Here the ratio of MDSB to (SSB + DSB) yields increases from about 0.01 near 35−40 eV to 0.06 near 100 eV, indicating the increasing probability for multiple DSBs being formed in one plasmid, while the probability for single SSB or DSB formation remains constant. It is interesting to note that this roughly 2 orders of magnitude difference, observed here, is similar to the difference in cross sections between ionizations yielding single (reaction 4 or 5) and multiple cation fragments (reaction 6) in gas phase electron−molecule collisions.[29] Thus, even if the MDSBs would exclusively involve interactions of secondary electrons, produced here in the plasmid by the higher incident beam electrons, they occur with small probability. Nonetheless, despite this small probability, if MDSBs occur in cellular DNA, they would be significantly more lethal than single SSBs or DSBs, since even if repaired by the cell they would likely result in large deletions of the DNA primary sequence.

## Summary and Conclusions

The present measurements show that, for electron energies below 15 eV, formation and decay of transient anion states, i.e., resonances, within DNA is the dominant mechanism leading

(44) Fain, B.; Rudnick, J. *Phys. Rev. E* **1999**, *60*, 7239−7252.

(45) Carlson, T. A.; White, R. M. *J. Chem. Phys.* **1966**, *44*, 4510.
(46) Souda, R. *Surf. Sci.* **2002**, *511*, 147.
(47) Souda, R. *J. Chem. Phys.* **2002**, *116*, 8556.

to SSBs and DSBs; this is characterized by a threshold near 4−6 eV and a strong maximum at about 10 eV in the electron energy dependence for both. The resonances are proposed to be localized on the different individual components of the DNA plasmid and clearly relate to some of the resonances measured in gas or condensed phase electron impact experiments on DNA bases, deoxyribose analogues, water, and short single stranded oligomers. Conversely, above 15 eV electron energy the SSB and DSB yields appear to be dominated by a superposition of various nonresonant mechanisms related to excitation, ionization, and dissociation of neutral or cationic excited states, as well as some small contribution from multiple scattering EEL of the incident higher energy electron, followed by subsequently induced strand break formation. Whereas below 15 eV incident electron energy, secondary electrons produced by the incident beam electrons do not contribute to the strand break yields, above 30 eV they are estimated to contribute at most 20−25% to the SSB or DSB yields measured at the highest incident electron energies, in the present thin film experiments.

With the exception of the MDSB yields below 40 eV, which are almost an order of magnitude lower than the combined SSB and DSB yields, the strand break yields in the present thin film experiments are the result of single incident electron events. Below 40 eV the MDSB yields may contain contributions from multiple electron damage to the same DNA molecule; however, at 40 eV and above, the MDSB yields are likely the result of sequential energy deposition events (nano-tracks) by a single incident electron at sites that are distant in primary sequence within the plectonemically supercoiled plasmid, but are in close contact with each other.

In irradiated bulk media, such as cells, nonthermal secondary electrons with initial energies below 15 eV greatly outnumber those with higher energies[2−4] almost 10 to 1; thus, our present results strongly suggest that nascent DNA damage induced by these abundant secondary electrons is dominated by mechanisms involving localized molecular resonances similar to those observed here or in basic constituents of DNA. Much like molecular excitation or ionization, the fundamental resonant mechanisms involved here are universally observed (or observable) in any molecule, in almost any state of aggregation,[48] albeit somewhat modulated by the particular physical and chemical environment, in the present case the DNA plasmid. Thus, they are expected to occur in living cells as well, and a full understanding of the biological effects of ionizing radiation must incorporate detailed knowledge of their action, including the nascent reaction cascades they induce (e.g., ion and radical reactions) along radiation tracks.

**Acknowledgment.** This work is supported in part by individual research grants (M.A.H., D.H., and L.S.) from the Canadian Institutes of Health Research (CIHR), as well as a CIHR group core-grant (CIHR Group in Radiation Sciences).

JA029527X

(48) Christophorou, L. G., Illenberger, E., Schmidt, W., Eds. *Linking the Gaseous and Condensed Phases of Matter: the Behaviour of Slow Electrons*; Nato ASI Series B; Physics Vol. 326; Plenum: NY, 1994.